Study on the influence of ethanol addition on exhaust gas composition and soot formation in iso-octane flames

I. Frenzel[*,1], D. Trimis[2,1]

[1]TU Bergakademie Freiberg, Institute of Thermal Engineering, Freiberg, Germany
[2]Karlsruhe Institute of Technology, Engler-Bunte-Institute, Division of Combustion Technology, Karlsruhe, Germany

Abstract
The emphasis of the work was to study soot formation in the combustion process of various iso-octane/ethanol blends. Selected exhaust gas species and soot particle size distributions at different heights above the burner were measured in selected fuel-rich atmospheric pressure laminar premixed iso-octane/ethanol flames. The results showed that the addition of ethanol to the reference fuel iso-octane reduces both the concentration of the gaseous soot precursor acetylene and the soot formation potential in the exhaust gas of the flames. The comparison of the soot particle size distributions indicated that both the process of soot particle nucleation in the lower heights of the flame and coagulation in the larger heights of the flame are influenced by the positive effect of the addition of the oxygenated fuel.

Introduction

The legislation for soot particle emissions has become stricter by limiting not only the mass but also the total number of particles. At the same time the use of biofuels in gasoline engines is of increasing importance to reduce the global CO_2 emissions. For spark-ignition engines renewable bio-ethanol is mainly used for blends and different blends of bio-ethanol and conventional fossil fuels having mixing ratios in the range of E5 to E85 are available for commercial automotive applications [1, 2, 3].

However, the different physical and chemical properties of the bio-components in the fuel have a high impact on the combustion process in engines and affect the soot formation and therefore the soot particle emissions from vehicles as well. In general, the addition of ethanol to the fuel reduces the particle emissions [4, 5], but in other studies contradictory trends were observed [6, 7]. However, these global analyses with special engine geometries and operating points do not allow general statements regarding the soot particle emissions. Due to the complex behavior of the fuel mixtures there is a leak of knowledge in the engine combustion process chain and therefore a forecast of soot formation for single fuels and operating conditions is still not possible.

In this work pure iso-octane, known as primary reference fuel in engine combustion research, was used as reference fuel and the influence of ethanol addition was studied in detail to investigate the underlying physical and chemical phenomena leading to the differences in soot formation when ethanol is added. The investigations were carried out under simplified conditions in lab-scale flames to obtain experimental data without the influence of the complex interactions in an engine and therefore to provide data for modeling purposes.

The influence of ethanol addition on flame structure, exhaust gas composition and soot formation in the premixed lab-scale combustion of several short-chain hydrocarbon fuels has been already studied by different groups. Wu et al. [8] and Salamanca et al. [9] investigated premixed laminar ethylene flames in a flat-flame burner and observed that the addition of ethanol reduces the soot particle formation. Additionally, Wu et al. showed that the concentration of gaseous soot precursors and polycyclic aromatic hydrocarbons (PAH) in the exhaust gas of the flames are lower when ethanol is added to the fuel. These observations were confirmed by the work of Gerasimov et al. [10] that studied the effect of ethanol addition on the species pool in ethylene flames experimentally and by chemical kinetic modeling. Furthermore, the experimental and modeling work of Bierkandt et al. [11] showed that the soot precursor concentration is reduced when ethanol is added to a premixed flat acetylene flame.

However, no experimental data is available for the influence of ethanol addition on soot formation in flat flames of higher hydrocarbons such as iso-octane. Therefore the emphasis of this work was to investigate various iso-octane/ethanol blends and to analyze the influence of ethanol addition on exhaust gas composition with the focus on gaseous soot precursors and soot particle formation in detail.

The utilized experimental setup consisted of a McKenna burner [12] and a suitable system for supplying and conditioning of fuel and oxidizer. Soot particle size distributions were measured at different heights above the burner (HAB) in selected fuel-rich atmospheric pressure laminar premixed iso-octane and ethanol flames, as well as from iso-octane/ethanol blends E20, E40, E65 and E85 flames with a constant equivalence ratio of $\phi = 2.3$ using an in situ probe sampling and a suitable gas conditioning system (similar to [13]) for online analysis with a scanning mobility particle sizer (SMPS). Additionally, axial concentration profiles of the major exhaust gas species and gaseous soot precursors, e.g. acetylene, were obtained from the analysis by a gas chromatograph after suitable sampling and conditioning of the exhaust gas from the flames.

[*] Corresponding author: Isabel.Frenzel@iwtt.tu-freiberg.de

Experimental Setup and Method

The experimental setup used in this study is described in the following and is schematically shown in Figure 1. The investigated flames were stabilized on a commercial McKenna burner (provided by *Holthius & Associates* [12]) that consists of an inner sintered porous bronze plug (inner diameter 60 mm) and an outer concentric annulus for shroud nitrogen (flow rate 10 ln/min) shielding the flame from the atmosphere. Due to the on-going investigations with liquid fuels the common water cooling of the burner plate was changed to a cooling with oil. To avoid condensation in the burner plate, the recirculating oil temperature was fixed at 353 K. A stabilization plate made of stainless steel was placed 50 mm above the burner plate to further stabilize the flames.

The conditions of all studied flames are summarized in Table 1. In addition to the iso-octane/ethanol blends E20, what means 20 vol.-% of liquid ethanol in iso-octane, E40, E65 and E85, pure iso-octane and ethanol were used as fuels as well. The equivalence ratio was fixed at ϕ = 2.3 for all investigated iso-octane/ethanol flames and the superficial cold gas velocity of the unburnt gas mixture of all flames was 5 cm/s at 273 K and 1 atm (in an empty cylinder of the same diameter).

The oxidizer mixture contained oxygen (purity 99.999%) and argon (purity 99.999%) as diluent. The oxygen content in the oxidizer mixture was set to 29 vol.-% due to flame stability requirements. The nitrogen used as shroud gas and as dilution gas for the sampling of the soot-loaden exhaust gas has a purity of 99.8%. All gases were supplied via *Bronkhorst* thermal mass flow controllers and the liquid iso-octane (purity 100%) and/or liquid ethanol (purity 99.9%) via *Bronkhorst* Coriolis mass flow controllers which cause uncertainties on the resulting equivalence ratio of maximum $\Delta\phi$ = ±0.03.

Initially the liquid fuel was stored in the upper part of a piston accumulator and pressurized with nitrogen to 5 bar(g), that was applied at the lower side of the accumulator so that there was no direct contact of the two fluids and thus unwanted dissolving of nitrogen in the liquid fuel was avoided. The flow of the liquid fuel was set by the Coriolis mass flow controller and was evaporated in an adapted direct evaporator type aSTEAM from *aDROP GmbH* afterwards. The main advantages of this evaporator are the pulsation free conversion of the liquid into the gas phase and that no carrier gas is needed what simplifies the experimental control. The working temperature of the evaporator was set to 513 K in order to provide most stable operation in respect to the applied mass flow and specific evaporation enthalpies.

Table 1. Flame conditions.

Fuel	ϕ	Unburned mole fraction of mixture x_i			
		C_8H_{18}	C_2H_5OH	O_2	Ar
E0	2.3	0.0507	-	0.2753	0.6740
E20	2.3	0.0422	0.0303	0.2690	0.6585
E40	2.3	0.0331	0.0632	0.2621	0.6417
E65	2.3	0.0204	0.1086	0.2526	0.6184
E85	2.3	0.0092	0.1490	0.2441	0.5977
E100	2.3	-	0.1819	0.2373	0.5808

In order to create a homogenous mixture of the vaporized fuel and the already preheated (373 K) gaseous mixture of oxygen and argon a preheated mixing chamber, which prevents the condensation of evaporated iso-octane and/or ethanol during mixing, was used. The temperature of the fuel/oxidizer mixture at the inlet of the burner was fixed at 353 K. Furthermore, all transport lines downstream the mixing chamber, the burner itself and the shroud nitrogen were

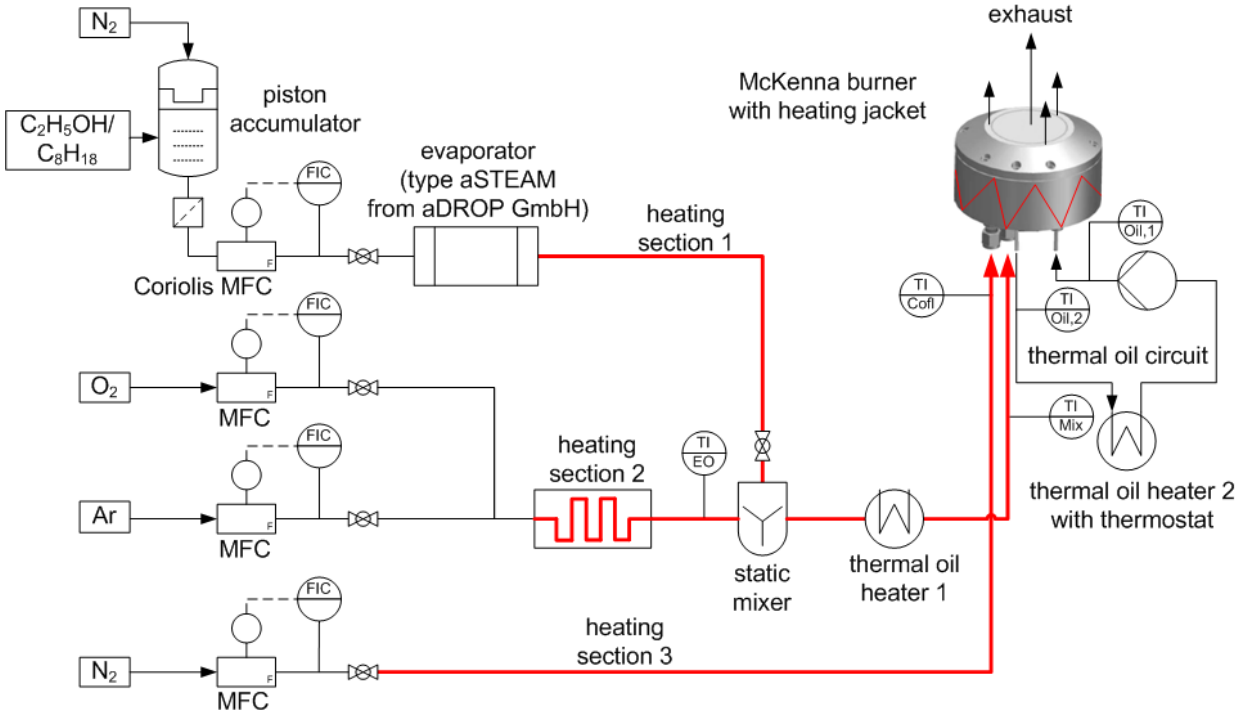

Figure 1. Schematic of experimental setup.

preheated up to minimum 353 K as well to avoid condensation of the evaporated ethanol on cold surfaces.

The realized soot particle sampling system is shown in Figure 2 and was similar to the one of Zhao et al. [13]. A ceramic sample probe tube (made of Al_2O_3 > 99.5%, inner diameter 9 mm, outer diameter 10 mm) was placed horizontally above the burner. The sample orifice with a diameter of 0.3 mm was drilled in the middle of the probe tube and positioned along the centerline of the flame, facing downward towards the incoming burning gas. The chosen orifice diameter was found to be the best compromise between the achievable dilution ratio at a stable pressure difference over the orifice and the time for clogging of the orifice. However, the orifice was cleaned after every scan with a 0.25 mm diameter wire. To draw the soot containing gas sample through the orifice, a small vacuum was realized in the sampling tube. The particle-loaden gas stream was diluted immediately by a particle-free nitrogen flow at room temperature (30 ln/min) resulting in a quenching to a temperature of around 315 K. The dilution ratio (DR) of the resulting turbulent flow (mean Reynolds number Re = 5000) in the sampling probe was DR > 10^4.

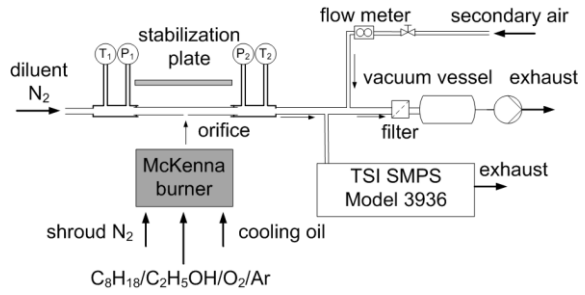

Figure 2. Schematic of gas sampling and conditioning system for soot measurements.

This dimension was reported to be necessary in order to prevent particle losses caused by coagulation and diffusive wall deposition in the sampling line [13, 14, 15]. For the dilution system used in this work, this finding could be confirmed, as the soot particle size distributions were found to be independent from the applied dilution ratio for DR > 10^4.

After the probe tube, the sample flow was split into two streams, a small portion of 1.5 ln/min entering the SMPS (metered by an impactor (0.071 cm nozzle)) and a large portion exhausted by a pump. In order to regulate the pressure in the sample probe and thus to adjust the applied dilution ratio, a secondary clean air stream with adjustable flow rate was introduced. The resulting dilution ratio in this study was chosen to be DR ~$2 \cdot 10^4$, leading to an unavoidable uncertainty of < ±24%. Further information concerning the estimation of the dilution ratio from the pressure difference across the orifice can be found in [13]. The applied dilution ratio was proved to be right measuring and comparing the CO concentrations in the undiluted and the diluted exhaust gas of an ethylene flame within the framework of preliminary investigations. The mean residence time of the highly diluted sample from the probe orifice to the SMPS inlet was approximately 420 ms.

The soot particle size distributions were measured with a commercial SMPS (*TSI* Model 3936) which consists of a Kr-85 bipolar charger, a nano differential mobility analyzer (nano-DMA *TSI* Model 3085) and a condensation particle counter (CPC *TSI* Model 3775). This equipment enables the measurement of mobility particle diameters in the range of 2 to 66 nm. However, the smallest reliably detectable particle size was 4 nm (counting efficiency higher than 50%). Using the parameterized correlation between the mobility diameter and the particle diameter of a carbonaceous particle from [16, 17], the measured mobility particle diameters were transformed into physical particle diameters to compare them directly with the numerical results. A scan-up time of 60 s and a retrace time of 20 s were utilized for the measurements.

The resulting size distribution measurements were corrected for particle losses via diffusion in the transport line from the sample probe orifice to the SMPS inlet [18] and for diffusion losses and multiple charges within the SMPS system. Finally, at least three samples of each flame were measured and a mean size distribution was calculated in order to correct statistical discordant values.

The McKenna burner itself was mounted on a vertical traversing system in order to adjust the distance between sampling orifice and burner surface. The different heights above the burner correspond to different residence times and thus the progress of the chemical reactions can be followed by performing measurements at different heights above the burner. A horizontal traversing system was used to allow access to the orifice in the sampling probe for regularly cleaning of the same. The accuracy of both the vertical and the horizontal positioning was better than ±0.02 mm.

To provide the axial temperature profiles of the investigated flames, flame temperature measurements were conducted using a type S sheath thermocouple with a diameter of 0.5 mm, coated with Mg-PSZ to avoid catalytic effects on the thermocouple tip during temperature measurement in the flame. The measured axial temperature profiles were corrected for radiation losses subsequently [19] and the error in the measured temperature was maximum ±80 K.

To analyze the exhaust gas composition of the studied flames and create axial species concentration profile exhaust gas was sampled from the flame at different axial positions using a quartz glass probe with an inner diameter of 1.2 mm. The gas flow through the probe was created via a membrane pump and the hot exhaust gases where cooled down to a temperature of approximately 373 K immediately after sampling from the flame to quench unwanted chemical reactions in the gas sample. A gas chromatograph by *Thermo Scientific* including both a flame ionization detector for the analysis of hydrocarbons and a thermal conductivity detector for permanent gases was used to get the dry composition of the sampled exhaust gases. Each gas

sample was measured three times and the average of these three values is shown in the graphs. The species mole fraction values have maximum uncertainties of ±10%. Although major species, e.g. hydrogen, carbon monoxide, carbon dioxide, etc. and hydrocarbons, e.g. methane, ethylene, acetylene, etc. in the exhaust gases of the studied flames were measured, only the axial profiles of the gaseous soot precursor acetylene are presented and discussed here exemplarily due to its important role in the soot formation process.

Results and Discussion

Pure iso-octane and ethanol

First the flame temperature, exhaust gas composition and soot formation in pure iso-octane and ethanol flames were examined. In Figure 3 selected measured particle size distribution functions (PSDFs) of soot sampled from the iso-octane (E0, top) and ethanol (E100, bottom) flames at different representative HABs are presented. The corresponding total number densities (bottom), soot volume fractions (middle) and the measured flame temperatures (top) are plotted in Figure 4 as function of HAB.

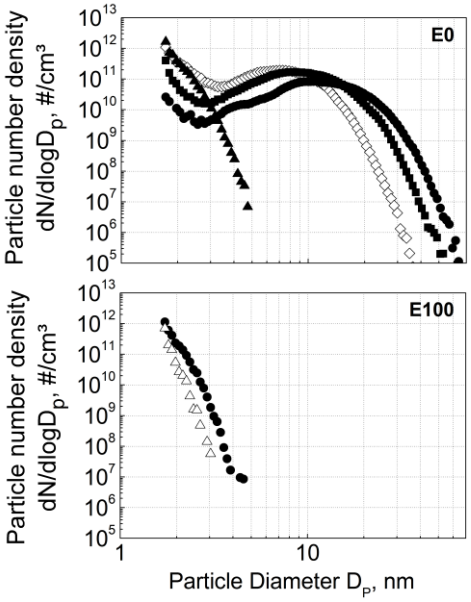

Figure 3. Variation of PSDFs in E0 (top) and E100 (bottom) flames (ϕ = 2.3) at different HABs (4 mm (▲), 6 mm (◊), 8 mm (■), 10 mm (Δ), 12 mm (●).

The first stable and reproducible PSDF in the iso-octane flame was measured at HAB = 4 mm and shows the characteristic shape of a particle nucleation mode with a maximum particle diameter of 4.7 nm. Further in the flame (HAB = 6 mm) a shoulder starts to grow out and the distribution becomes bimodal. The nucleation mode remains indicating sustained particle nucleation. For particle sizes larger than 3 nm the PSDF is very close to a log-normal distribution with a median diameter of 12 nm and a maximum diameter of 65 nm. As can be expected from the PSDFs, the soot volume fraction increases exponentially over the entire distance measured and reached a value of $5.1 \cdot 10^{-8}$ at HAB = 12 mm. The total number density shows the often observed "first rise, then fall" behavior. The initial rise caused by particle nucleation is followed by the maximum of around $2.9 \cdot 10^{11}$ at HAB = 5 mm and levels off later in the flame due to balanced coagulation and particle nucleation in the upper flame region.

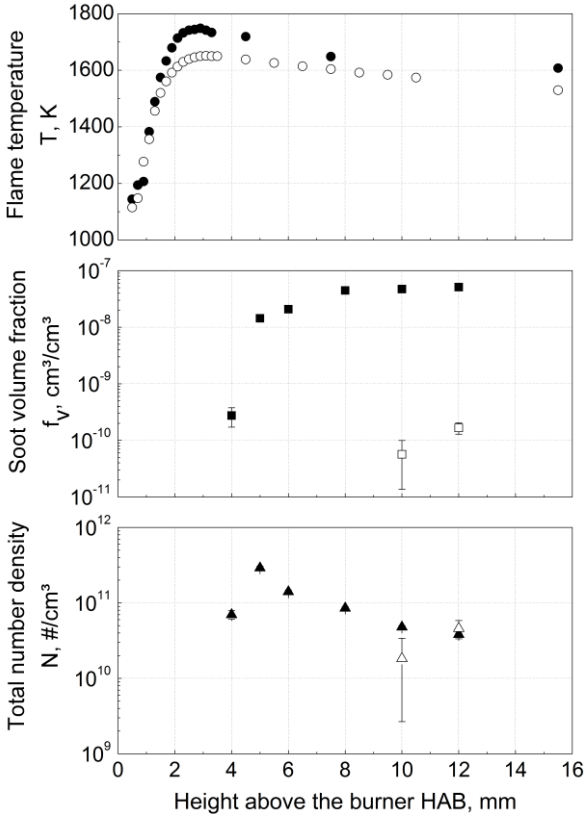

Figure 4. Radiation-corrected axial flame temperature profile (top), soot volume fraction (middle) and total number density (bottom) in E0 (filled symbols) and E100 (open symbols) flames (ϕ = 2.3).

The PSDFs sampled from the pure ethanol flames and shown in the lower graph of Figure 3 already indicate clearly that the ethanol flame is a slightly sooting flame and therefore much less soot is produced in comparison to the iso-octane flame while the conditions of the flame such as equivalence ratio and cold gas velocity were the same. The first soot was detected at HAB = 10 mm and it can be observed that soot inception is dominant. The comparison of the soot volume fractions of the iso-octane and the ethanol flames shows that the value for the iso-octane flame is two orders of magnitudes higher than the one for the ethanol flame, whereas the total number densities are in the same order of magnitude.

In Figure 5 the mole fractions of the gaseous soot precursor acetylene in the dry exhaust gas of the iso-octane and the ethanol flames are shown for different HABs in the range of 1 mm to 7 mm. The comparison of these two profiles confirms the finding that the iso-

octane flame generates much more soot than the ethanol flame. The mole fraction of acetylene in the exhaust gas of the iso-octane flame is 1.5 fold higher than in the ethanol flame for the lower HABs and only at HAB = 7 mm they reach almost the same value.

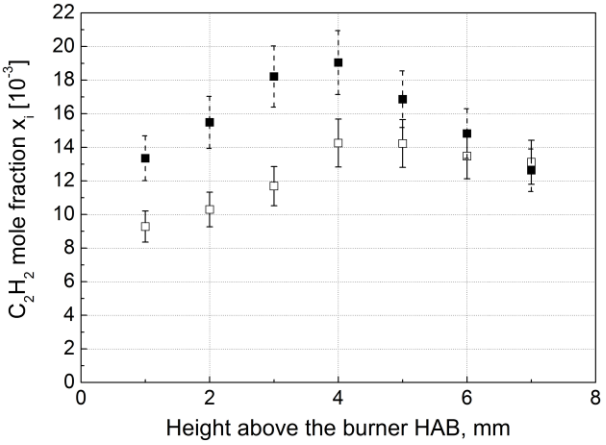

Figure 5. Mole fraction profiles of acetylene in the dry exhaust gas of E0 (filled symbols) and E100 (open symbols) flames (ϕ = 2.3).

Blends of iso-octane and ethanol

In Figure 6 the PSDFs of soot sampled from four different iso-octane/ethanol blends at three representative heights above the burner, HAB = 6 mm, 8 mm and 12 mm, are presented. Additionally the already discussed PSDFs of the pure iso-octane and ethanol flames are shown as well. PSDFs could not be measured for all blends at all HABs, especially for the low HAB of 8 mm, due to the fact that the process of soot particle nucleation starts later in the flame with increasing amount of ethanol in the fuel. First stable and reproducible PSDFs in flames of E20 could be measured at HAB = 5 mm, however, in the E85 flame only at HAB = 8 mm. This confirms the findings of Salamanca et al. [9] explaining that ethanol addition to a hydrocarbon fuel slows down the mechanism of nanoparticle formation in the flames. Higher residence times are needed for particle nucleation and consequently also the process of coagulation starts later in the flame.

As can be seen in Figure 6 a shift of the PSDFs to smaller diameters occurs with increasing ethanol content in the fuel and the bimodal distributions for E0, E20 and E40 become unimodal for E65 at HAB = 6 mm. At HAB = 12 mm the PSDFs of E0, E20 and E40 are similar and just a high amount of ethanol in the fuel (> E65) reduces significantly the soot formation. The addition of ethanol leads to the disappearance of large soot particles and therefore of the soot particle growth mode in the PSDF, but only to a slight decrease of the amount of very small particles. The measured PSDFs of the soot sampled from all studied flames show clearly that the amount of small nanoparticles with diameters <5 nm is high and is not much influenced by ethanol addition. These particles do not contribute significantly to the total soot mass emitted but are mainly responsible for the total particle number density.

Salamanca et al. [9, 20] observed the same effect during their experimental investigations with premixed ethylene/ethanol flames and stated that the reason for the selectivity of ethanol in reducing particles on the basis of their size is the slow-down of the coagulation process leading to soot. The bonded oxygen in the ethanol enhances the fuel oxidation and therefore PAH and precursor nanoparticle formation are reduced. Therefore the following process of soot formation by coagulation and surface addition on the particle nuclei is less effective.

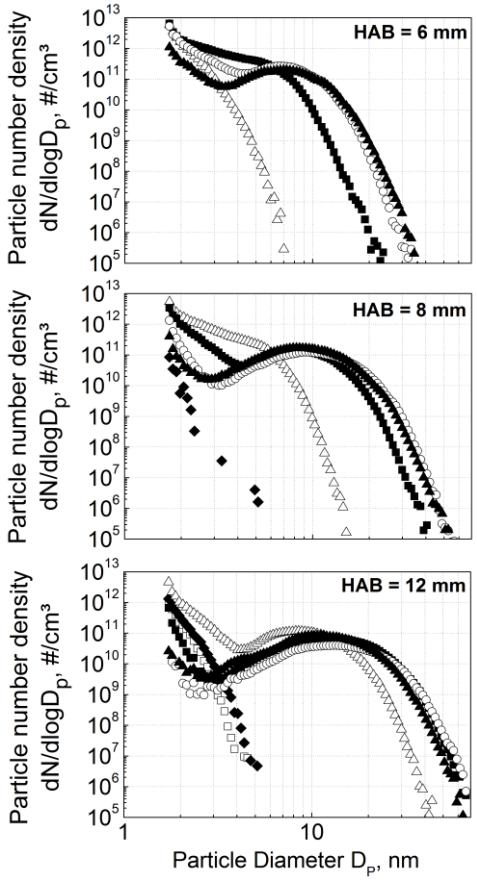

Figure 6. Variation of PSDFs in E0 (▲), E20 (○), E40 (■), E65 (Δ), E85 (♦) and E100 (□) flames (ϕ = 2.3) at three different HABs.

Figure 7 summarizes the soot volume fractions of all six studied flames at different HABs and shows a general reduction of the total volume fraction of soot when ethanol is added, with an increasing reduction as a function of the amount of ethanol added. Up to E40 the reduction is prominent just for low HABs and at HAB = 10 mm the differences in the soot volume fractions of E0, E20 and E40 are within the measurement accuracy. However, for the fuels E65, E85 and E100 the reduction of the soot volume fraction compared to pure iso-octane E0 is prominent for all HABs. The reason for this effect is that in highly sooting flames like the studied iso-octane flame surface reactions control the final amount

of soot and therefore the role of ethanol addition on the reduction of soot is less effective. In slightly sooting flames like the E85 flame the effect is more evident due to the fact that the inception process controls the final amount of soot [20].

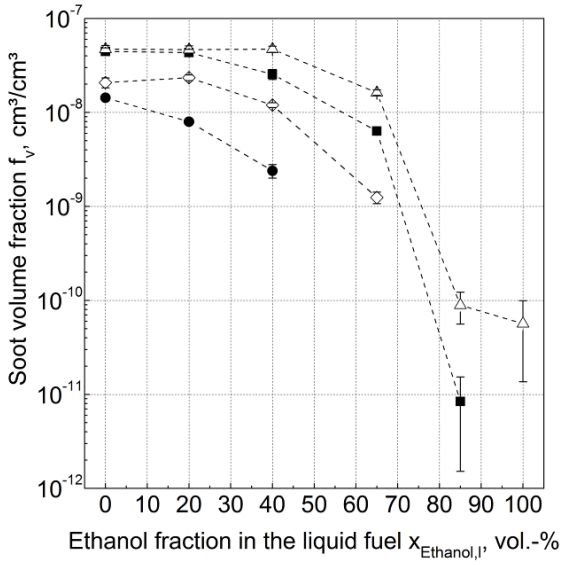

Figure 7. Variation of soot volume fractions in E0, E20, E40, E65, E85 and E100 flames at four different HABs (5mm (●), 6 mm (◊), 8 mm (■), 10 mm (Δ)).

Conclusions

Combustion soot formed in fuel-rich laminar premixed iso-octane/ethanol flames was quantitatively characterized by probe sampling followed by particle sizing using an SMPS. The experimental work focused on the detailed understanding of how the addition of ethanol to the reference fuel iso-octane influences the soot formation process and especially the soot particle size distribution. The results show that the ethanol addition reduces both the concentration of gaseous soot precursors in the exhaust gas of the flame and the soot formation potential. The comparison of the soot particle size distributions of iso-octane, ethanol and the investigated blends for the same flame conditions indicates that both the process of soot particle nucleation in the lower heights of the flame and the coagulation process in the larger heights are influenced by the positive effect of the addition of the oxygenated fuel. This results in a reduction of the total soot volume fraction and the soot particle diameter, however, not significantly in a decrease of the total particle number. Very small soot particles have a stronger effect on health compared to larger soot particles and therefore the addition of high amounts of biofuels like ethanol to a fossil fuel might lead to new difficulties especially concerning the soot formation in the combustion process.

Acknowledgements

The authors gratefully acknowledge the financial support by the Federal Ministry of Food and Agriculture in the project "Bildung von Rußpartikeln und katalytische Filterregeneration bei der motorischen Nutzung von Ottokraftstoffen aus Biomasse" (project number 22041111).

References

[1] Renewable energy directive 2009/28/EC RED (2009).
[2] B. Endo, Full scale bio-fuel popularization project. International Renewable Energy Agency; 2012.
[3] C. Hammel-Smith, J. Fang, M. Powders, J. Aabakken, Issues associated with the use of higher ethanol blends, National Renewable Energy Laboratory, 2002.
[4] J. Lee, R. Patel, A. Schönborn, N. Ladommatos, C. Bae, Energy and Fuels 23 (2009) 4363–4369.
[5] J. P. Szybist, A. D. Youngquist, T. L. Barone, J. M. Storey, W. R. Moore, M. Foster, K. Confer, Energy and Fuels 25 (2011) 4977–4985.
[6] L. Chen, R. Stone, Energy and Fuels 25 (2011) 1254–1259.
[7] R. Daniel, H. Xu, C. Wang, D. Richardson, S. Shuai, Applied Energy 105 (2013) 252–261.
[8] J. Wu. K.H. Song, T. Litzinger, S.-Y. Lee, R. Santoro, M. Linevsky, M. Colket, D. Liscinsky, Combustion and Flame 144 (2006) 675-687.
[9] M. Salamanca. M. Sirignano, M. Commodo, P. Minutolo, A. D'Anna, Experimental Thermal and Fluid Science 43 (2012) 71-75.
[10] I.E. Gerasimov, D.A. Knyazkov, S.A. Yakimov, T.A. Bolshova, A.G. Shmakov, O.P. Korobeinichev, Combustion and Flame 159 (2012) 1840-1850.
[11] T. Bierkandt, T. Kasper, E. Akyildiz, A. Lucassen, P. Oßwald, M. Köhler, P. Hemberger, Proceedings of the Combustion Institute 35 (2015) 803-811.
[12] The McKenna Flat Flame Burner, Holthuis & Associates, P.O. Box 1531, Sebastopol, CA 95473.
[13] B. Zhao, Z. Yang, J. Wang, M.V. Johnston, H. Wang, Aerosol Sci. Technol. 37 (2003) 611-620.
[14] B. Öktem, M.P. Tolocka, B. Zhao, H. Wang, M.V. Johnston, Combustion and Flame 142 (2005) 364 – 373.
[15] M. Maricq, S.J. Harris, J.J. Szente, Combustion and Flame 132 (2003) 328 – 342.
[16] J. Singh, R.I. Patterson, M. Kraft, H. Wang, Combustion and Flame 145 (2006) 117 – 127.
[17] B. Zhao, Z. Yang, Z. Li, M.V. Johnston, H. Wang, Proceedings of the Combustion Institute 30 (2005) 1441 – 1448.
[18] W. Hinds, Aerosol Technology, Wiley, New York (1999).
[19] C.Shaddix, Correcting thermocouple measurements for radiation loss: a critical review, Proceedings of the 33rd National Heat Transfer Conference (1999).
[20] M. Salamanca, M. Sirignano, D'Anna, Energy Fuels 26 (2012) 6144-6152.